

## EXPERIMENTAL INVESTIGATION OF THERMOPHYSICAL PROPERTIES AND HEAT TRANSFER CHARACTERISTICS OF HYBRID NANOFLUIDS BASED ON PARTICLE SIZE

by

**Ratchagaraja DHAIRIYASAMY<sup>a\*</sup>, Mohamed H. AHMED<sup>b,c</sup>,  
Yasser ABDELRHMAN<sup>c</sup>, Asif AFZAL<sup>d,e</sup>, Fadl A. ESSA<sup>f</sup>,  
Mishal ALSEHLI<sup>g</sup>, Ayman A. ALY<sup>h</sup>, and Bahaa SALEH<sup>g</sup>**

<sup>a</sup>Department of Mechanical Engineering, University College of Engineering, Villupuram, Tamilnadu, India

<sup>b</sup>Mechanical Engineering Department, King Abdulaziz University, Jeddah, Saudi Arabia

<sup>c</sup>Mechanical Engineering Department, Faculty of Engineering, Assiut University, Assiut, Egypt

<sup>d</sup>Department of Mechanical Engineering, P. A. College of Engineering

(Affiliated to Visvesvaraya Technological University, Belagavi), Mangaluru, India

<sup>e</sup>Department of Mechanical Engineering, School of Technology, Glocal University, Delhi-Yamunotri Marg, SH-57, Mirzapur Pole, Saharanpur District, Uttar Pradesh, India

<sup>f</sup>Mechanical Engineering Department, Faculty of Engineering, Kafrelsheikh University, Kafrelsheikh, Egypt

<sup>g</sup>Mechanical Engineering Department, College of Engineering, Taif University, Taif, Saudi Arabia

Original scientific paper

<https://doi.org/10.2298/TSCI210706005D>

*In heat transfer applications, nanofluids are utilized to increase thermal conductivity and heat transfer coefficient. The difficulty of nanoparticle stabilization in the fluids is a significant problem in heat transfer applications. Heat exchanger materials may wear and erode as a result of the additional nanoparticle. When compared to mono nanofluids, this can be lowered by using hybrid nanofluids. In this work, hybrid nanofluids are used in a radiator under laminar flow at 75 °C, and the effect of volume concentration on heat transfer enhancement is investigated. The thermophysical characteristics of hybrid nanofluids are investigated using SiC and Al<sub>2</sub>O<sub>3</sub> at 0.1 vol.% and 0.2 vol.%. The results revealed that a hybrid nanofluid with a higher volume concentration improves heat transfer. Finally, regression analysis for laminar flow is carried out and correlations for experimental Nusselt number and friction factor values were developed. The impact of particle size, flow rate, and temperature on the radiator's heat transfer enhancement is investigated using hybrid nanofluid at 75 °C. It is observed that the size of the nanoparticle has a substantial effect on heat transfer characteristics. It is concluded that using smaller-sized hybrid nanoparticles of Al<sub>2</sub>O<sub>3</sub>/SiC-S with less volume concentration enhances heat transfer and reduces radiator size compared to conventional coolants.*

**Keywords:** hybrid nanofluids, heat transfer coefficient, Nusselt number, friction factor, radiator

\*Corresponding author, e-mail: ratchagaraja@gmail.com

## Introduction

Coolant is the fluid that prevents a system from overheating by flowing through it to remove excess heat produced. It should have higher heat transfer characteristics, low viscosity cost. Besides these properties, it should not cause corrosion to the system while it is flowing. Conventional coolants cannot satisfy growing automotive cooling demand. Ethylene glycol (EG) and propylene glycol (PG) are used as coolants due to their antifreeze properties and higher boiling point. Corrosion and fouling are significant problems that damage the radiator system by using these coolants. The thermal conductivity and heat transfer performance is lower for these coolants. A new cooling fluid should be incorporated into automobiles to increase cooling performance at less cost to overcome these problems. Due to the increased thermophysical properties of the nanoparticles scattered in the base fluid, nanofluids improve heat transfer in the engine radiator. The size of the radiator can be lowered significantly when nanofluids are employed as a coolant in an automotive system, enhancing overall efficiency. The nanoparticles were used in combination with a base fluid such as water and EG. Recent studies have shown different methods for preparing nanofluid and stability analysis for various experimental investigations to analyse the thermophysical and heat transfer properties.

The  $\text{Al}_2\text{O}_3$  was utilized as a nanofluid in EG. with wire coil inserts for heat transfer enhancement in vehicle radiators by Goudarzi *et al.* [1]. With the usage of coils, a 9% increase in heat transfer was achieved, according to the findings. The parallel use of the coil inserts at concentrations of 0.08%, 0.5%, and 1% improved the thermal efficiency by 5% relative to coils' inserts alone. Devireddy *et al.* [2] used water as a coolant for an automotive radiator. They calculated the efficiency of  $\text{TiO}_2$  nanofluids based on EG. By increasing the fluid circulation rate, the heat transfer efficiency can be enhanced. Nanofluids have been shown to enhance heat transfer rates by up to 37% when compared to the base fluid. Elsebay *et al.* [3] used nanofluids instead of water flow to resize the radiator. Thermal and flow efficiency of two nanofluids ( $\text{Al}_2\text{O}_3$ -water and  $\text{CuO}$ -water) flowing into a flat radiator tube are tested. On the contrary, the required pumping capacity is increased over the base fluid after reducing the radiator volume.

Nieh *et al.* [4] employed  $\text{Al}_2\text{O}_3$  and  $\text{TiO}_2$  nano-coolant (NC) to improve the heat dissipation efficiency of an air-cooled radiator. The heat dissipation of the nanofluid was found to be higher than that of the base fluid in the experiments. It can be seen that  $\text{TiO}_2$  nanofluid outperforms  $\text{Al}_2\text{O}_3$  nanofluid. The overall improved ratio of heat dissipation efficiency, pressure decrease, and hydraulic strength are 25.6%, 6.1%, and 2.5%, respectively, compared to the base fluid. Thermal conductivity, viscosity, mass, and temperature of  $\text{Al}_2\text{O}_3$  nanoparticles dispersed in water and EG and utilized in automobile radiators were investigated by Elias *et al.* [5]. The thermal conductivity, viscosity, and density of the nanofluid significantly decrease as the volume concentrations increase. Hussein *et al.* [6] investigated the heat transfer improvement of an automobile radiator using  $\text{TiO}_2$  and  $\text{SiO}_2$  nanoparticles in pure water. The empirical results showed that  $\text{TiO}_2$  and  $\text{SiO}_2$  improved heat transmission with a vehicle radiator. For  $\text{TiO}_2$  and  $\text{SiO}_2$  nanofluids, the greatest increase in Nusselt numbers was 11% and 22.5%, respectively. Peyghambarzadeh *et al.* [7] used the traditional NTU technique to test the heat transfer efficiency of an automobile radiator. The  $\text{CuO}$  and  $\text{Fe}_3\text{O}_4$  nanoparticles are dispersed with water at 0.15 vol.%, 0.4 vol.%, and 0.65 vol.% concentrations with an appropriate pH. Both nanofluids had a greater heat transfer coefficient than water, according to the findings. The overall heat transfer coefficient improves as velocity, nanoparticle concentra-

tion, and nanofluid velocity increase. Vajjha *et al.* [8] statistically examined heat transfer using two distinct nanofluids,  $\text{Al}_2\text{O}_3$  and  $\text{CuO}$ , in an EG-water combination flowing through a radiator's flat tube to determine the nanofluids superiority over the base fluid. With increasing nanofluid volumetric concentrations, the friction factor and convective heat transfer effects improve. With varying nanofluid and Reynolds numbers, this presents quantitative implications of heat transfer coefficient and friction factor variations. Leong *et al.* [9] focused on the use of Cu nanofluids in a vehicle cooling system with EG. The overall heat transfer coefficient and heat transfer rate were enhanced when nanofluids were used as the base fluid instead of EG. Around 3.8% of the heat transfer improvement is realized with 0.2 vol.% Cu particles in the base fluid.

Jasim *et al.* [10] employed  $\text{Al}_2\text{O}_3$  nanofluid with 0.5% and 1% volume concentrations in a double pipe heat exchanger and observed that heat transfer improved as nanofluid volume concentrations and volume flow rates increased. In a double tube heat exchanger, Zhen *et al.* [11] investigated six nanofluids including  $\text{CuO}$ ,  $\text{Al}_2\text{O}_3$ ,  $\text{Fe}_3\text{O}_4$ ,  $\text{ZnO}$ ,  $\text{SiC}$ , and  $\text{SiO}_2$ . Due to its comparably high heat transfer performance and low friction factor, they found that  $\text{CuO}$ -water nanofluid offers a substantial benefit. Qamar *et al.* [12] investigated the stability and rheological characteristics of  $\text{ZnO}$  nanoparticles in deionized water and EG, finding that the viscosity increased with particle loading and surfactants had little effect. Under laminar flow conditions, Arulprakasajothi *et al.* [13] investigated the Nusselt number and friction factor behaviour in a tube heat exchanger with staggered and non-staggered conical strips, finding that the staggered conical strip with a twist ratio of  $Y = 3$  and 0.5% volume concentration of nanofluid provided the best heat transfer. Topuz *et al.* [14] investigated the thermophysical characteristics of  $\text{Al}_2\text{O}_3$ ,  $\text{TiO}_2$ , and  $\text{ZnO}$  nanofluids using deionized water and observed that their thermal conductivity is proportional to temperature. The viscosity is related to volumetric concentrations but inversely proportional to temperature at the same time.

It has been reported from the previous studies that the nanofluids used in the radiator showed enhancement of heat transfer characteristics. It is also noted that the Nusselt number is increased for all the nanofluids. The friction factor and pressure drop properties of nanofluids utilized in the radiator are also investigated. Apart from the aforementioned, some of the experiments conducted in automotive radiators with nanofluids to improve the heat transfer characteristics are given in tab. 1.

Due to the presence of various nanoparticles in the base fluid, it has been observed in the previous research that hybrid nanofluids provide higher heat transfer characteristics. The use of hybrid nanofluids would significantly increase the thermophysical characteristics and cooling rate compared to mono nanofluids. Due to the inclusion of various nanoparticles, particle aggregation is reduced in hybrid nanofluid. Compared to the enormous volume concentration of mono nanofluids, hybrid nanofluids have the same heat transfer properties. Many studies investigated the use of nanofluids to increase heat transfer coefficients and found that nanofluids had greatly improved heat transfer capacity due to their superior thermophysical characteristics. The  $\text{SiC}$  of large and small size nanoparticles is prepared with  $\text{Al}_2\text{O}_3$  in this experimental study. Experiments with various volume concentrations in laminar flow are carried out to determine the performance of a radiator. In this study, hybrid nanofluids are prepared at various volume concentrations. The effect of volume concentration and nanoparticle size on heat transfer properties for laminar flow at 75 °C in an automobile radiator is investigated.

**Table 1. Summary on nanofluids performance in automotive radiator**

Author	Nanoparticle /base fluid	Weight, w/ volume, $\phi$ [%]	Coolant flow conditions	Results and remarks
Selvam <i>et al.</i> [15]	Graphene nanoplatelets/water	0.1-0.5 vol.%	10-100 g/s	Enhancement of convective heat transfer coefficient of 0.5 vol.% than base fluid
Elsaid <i>et al.</i> [16]	Al <sub>2</sub> O <sub>3</sub> and Co <sub>3</sub> O <sub>4</sub> /DI water and EG	0.02 vol.%, 0.05 vol.%, 0.1 vol.%, 0.2 vol.%	0.05-0.2 kg/s	Nusselt number enhanced to 31.8% and the friction factor 16%
Cardenas <i>et al.</i> [17]	Graphene and Ag/DI water and EG	0.01 vol.%, 0.05 vol.%, 0.1 vol.%	0.08-0.11 kg/s	Increase of heat transfer rate by 4.4% for Ag
Kocak <i>et al.</i> [18]	Pure TiO <sub>2</sub> TiO <sub>2</sub> doped with 0.1% Ag TiO <sub>2</sub> doped with 0.3% Ag TiO <sub>2</sub> doped with 0.1% Cu/DI water and EG	0.3 vol.%, 0.5 vol.%, 1 vol.%, 2 vol.%	17-25 Lpm	Convection heat transfer coefficient increases for 0.3% Ag-doped TiO <sub>2</sub> nanofluids with concentrations of 1% and 2% is 26.15% and 27.72%
Singh <i>et al.</i> [19]	Copper oxide (CuO)/DI water	0.1-0.5 vol.%	Turbulent	Maximum heat transfer rate of 20% with 0.5% v/v
Tijani <i>et al.</i> [20]	Al <sub>2</sub> O <sub>3</sub> and CuO/DI water and EG	0.05 vol.%, 0.15 vol.%, 0.3 vol.%	3-6 Lpm	CuO nanofluid has a higher heat transfer coefficient than Al <sub>2</sub> O <sub>3</sub> nanofluid.
Moghaieb <i>et al.</i> [21]	Al <sub>2</sub> O <sub>3</sub> /DI water and EG	0.5 vol.%, 1 vol.%, 1.5 vol.%, 2 vol.%	1-2 m/s	A higher heat transfer coefficient of 78.67% at 1%
Oliveira <i>et al.</i> [22]	Multi-walled carbon nanotubes/DI water	0.05 wt.%, 0.16 wt.%	0.175 kg/s	Decrease in the heat transfer rate of 5%

### Materials and methods

The thermophysical characteristics of the base fluid should be improved by the nanoparticles dispersed in it. The thermophysical characteristics of nanoparticles vary with both volume concentration and temperature, as per the literature. The thermal conductivity of nanoparticles increases as the volume and temperature of the particles increase. Thermophysical properties increase as volume concentrations increase and decrease as temperature increases. As a result, the selection of base fluid is critical in the use of heat exchangers. The base fluid should not freeze, depending on the situation. De-ionized (DI) water, pure water, pure EG, and EG/DI water are all utilized as coolants in various proportions. The DI-water and EG are being used as base fluids in variable concentrations in this experiment. The base fluid in this study is a DI water/EG mixture with a 70% DI water volume concentration.

### Preparation of nanofluids

Silicon carbide (SiC) and Al<sub>2</sub>O<sub>3</sub> were used as the nanoparticles for this study. To decrease size, SiC with an average diameter of 90 nm is processed in a planetary ball mill. Because of the milling process, the size of SiC is decreased by 28%, resulting in a more amorphous output. The SiC particles had a w.% of 53.1 Si and 38.13 C after milling, with 10.87 w.% of Fe, as determined by EDS proportions.

The two-step approach for preparing nanofluid is used. The Al<sub>2</sub>O<sub>3</sub>/SiC-L and Al<sub>2</sub>O<sub>3</sub>/SiC-S are initially dispersed in DI water and EG at volume concentrations of 0.1 vol.%

and 0.2 vol.%, respectively. To ensure that the base fluid and nanoparticles are stable, sodium citrate is added as a stabilizer, and magnetic stirring is performed. Sonification is performed for 3 hours with continual stirring to minimize agglomeration in the fluid. Similarly, nanofluids with volume concentrations of 0.1 vol.% and 0.2 vol.% are generated for  $\text{Al}_2\text{O}_3/\text{SiC-S}$  and  $\text{Al}_2\text{O}_3/\text{SiC-L}$ , respectively. Both large and small nanoparticles are ultrasonicated with base fluid to obtain nanofluid without sedimentation in an ultrasonic bath as shown in fig. 1. The prepared nanofluids are monitored for 12 days showing good stability, as shown in fig. 2.



Figure 1. Ultrasonication bath

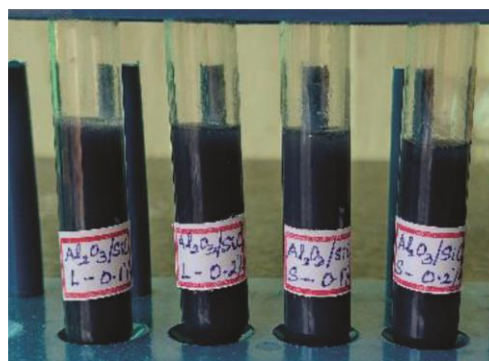


Figure 2. Prepared nanofluid

### **Morphology of nanofluids**

Hybrid nanofluids comprise two or more different particles in the base fluid regardless of particle size distributions or distinctive geometries. The morphology of the hybrid nanofluids of  $\text{Al}_2\text{O}_3$  and SiC is analysed using SEM with energy dispersive spectroscopy (EDS). The TEM image of the hybrid nanofluid is shown in fig. 3, proving the particles are spherical. Energy-dispersive X-ray spectroscopy is a widely used technique for determining the elemental compositions of extremely tiny material samples. The electron beam excites the atoms on the surface, producing particular wavelengths of X-rays that indicate the elements atomic structure. A concentrated beam of charged particles with high energy is directed into the sample under investigation. An X-ray with the energy of the difference in the binding energies of the electron levels is emitted when an electron from a higher binding energy electron level falls into the core hole. The EDS analysis generates a spectrum that contains peaks according to the sample's elemental makeup.

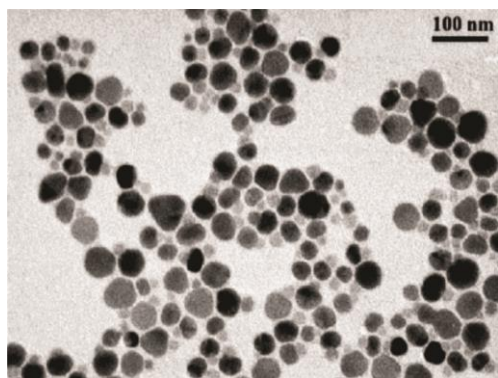


Figure 3. The TEM image of hybrid nanofluids

It is seen from fig. 4 that  $\text{Al}_2\text{O}_3/\text{SiC-L}$  is spherical with large agglomerates, and the image segmentation and particle size distribution ranges from 25 nm to 80 nm. Figure 5 showed that  $\text{Al}_2\text{O}_3/\text{SiC-S}$  with spherical shape contains more particles, and the distribution of particle size ranges from 10 nm to 25 nm. The EDS images of hybrid nanofluids of  $\text{Al}_2\text{O}_3$  with larger SiC are shown in fig. 6, and  $\text{Al}_2\text{O}_3$  with smaller SiC is shown in fig. 7, providing the presence of corresponding elements.

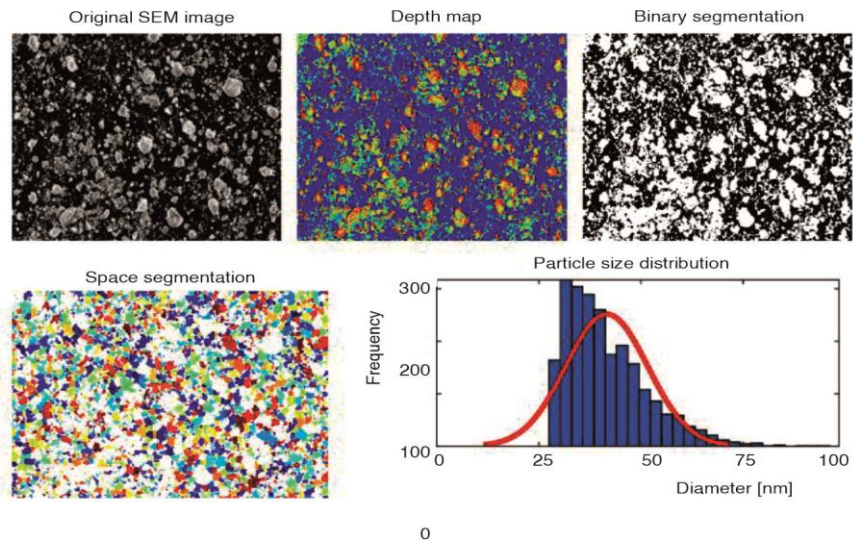


Figure 4. Particle size distribution of  $\text{Al}_2\text{O}_3/\text{SiC-L}$

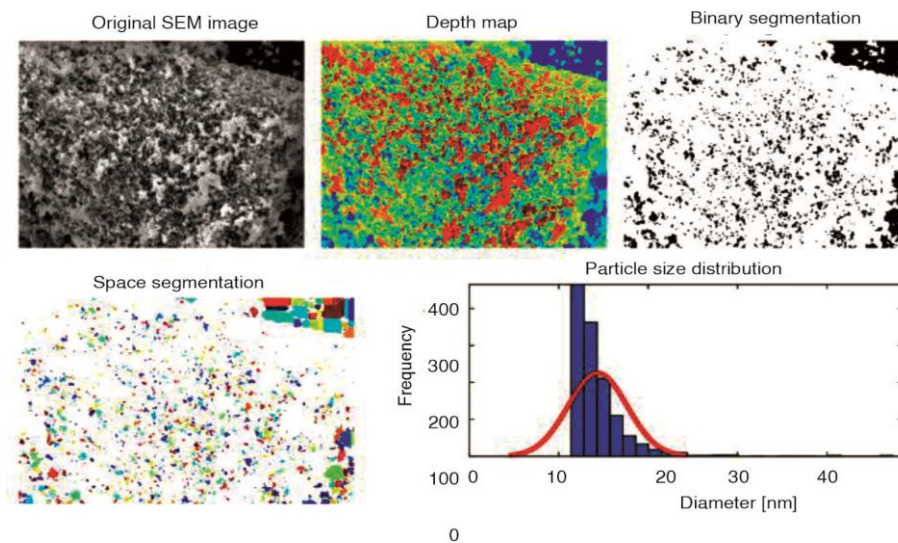


Figure 5. Particle size distribution of  $\text{Al}_2\text{O}_3/\text{SiC-S}$

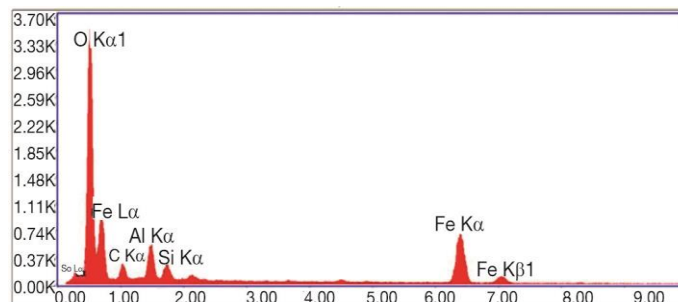


Figure 6. The EDS image of the  $\text{Al}_2\text{O}_3\text{-SiC-L}$

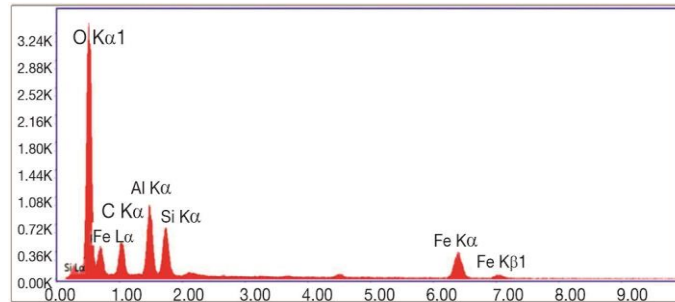


Figure 7. The EDS image of the  $\text{Al}_2\text{O}_3\text{-SiC-S}$

### Stability of nanofluids

The sedimentation of nanoparticles will influence the thermal conductivity of nanofluids in the base fluid. The zeta potential of the produced fluids is measured to determine nanofluid stability. The zeta potential of nanofluids during 16 days varies from 47-59 mV, as shown in fig. 8. This demonstrates that hybrid nanofluids are highly stable.

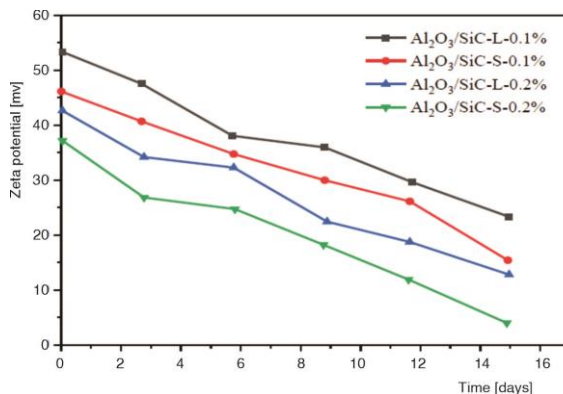


Figure 8. Stability analysis

The presence of a zeta potential greater than 32 mV, defined by the ASHRAE standard, indicates that the fluids are stable. The stability of the produced nanofluid is tested for 60 days (12 days intervals), indicating that no sedimentation has occurred. Compared to the larger particles in the base fluid, the nanofluid with smaller nanoparticles shows good stability. Even though the zeta potential falls with the number of days due to clusters created by particle agglomeration, the stability of the prepared nanofluids is more than 48 mV, demonstrating that nanofluids can be used for heat transfer applications.

### Experimental set-up and procedure

Figure 9 shows a photographic view of the experimental set-up. Vertical aluminium tubes with an induced draught fan constitute the radiator. The cross-flow design is used with the axial fan, which is fitted with a radiator that pulls air to cool the hot fluid moving through the system. The arrangement has two circuits: a hot fluid circuit and a cold air circuit. A heater with a thermostat, circulating pump, and flow meter control the fluid flow in the hot fluid system. An axial fan supplies cold air to the radiator in the cold air circuit.

Temperature sensors are installed on the radiators inlet and outlet, and the temperature is recorded using a data logger. The air velocity is measured with a digital anemometer. Two points control the feed temperature, and the PID power control unit is governed by the data acquisition software. The heater may also be manually regulated using a control variable ranging from 0-100%. With a safety group that restricts the pressure and automatic bleeding of the heating circuit will be supplied. Along with the radiator, an axial fan is installed to

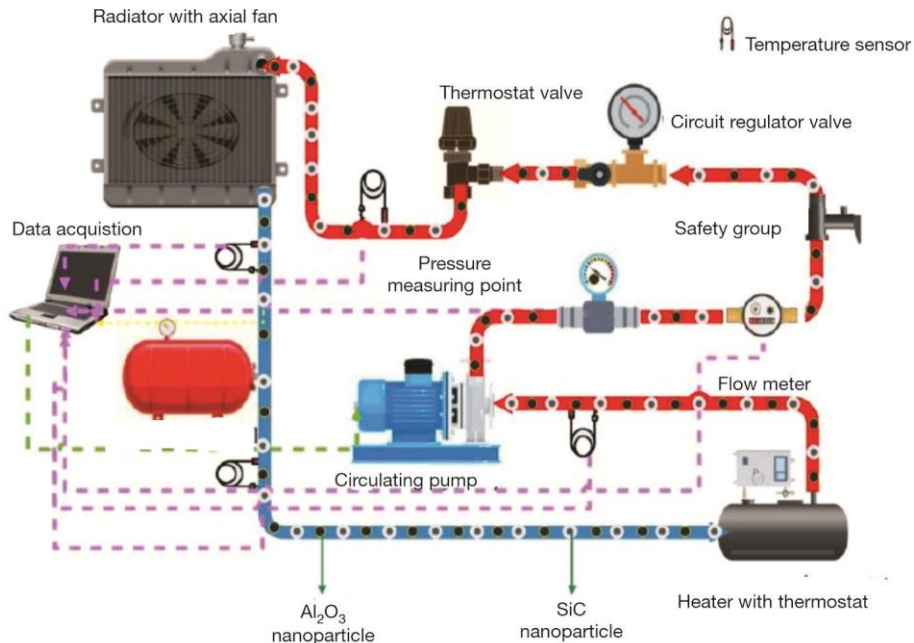


Figure 9. Photographic view of the experimental test set-up

disperse the heat. Water cannot be compressed as it expands during heating. To compensate for this expansion, vessels with a gas space are provided. The water level above the expansion vessel corresponds to the entry pressure of the gas space with hot water. In the radiator, the heat transfer characteristics are investigated at various flow rates. The effect of particle size on the base fluid is investigated using SiC nanoparticles of different sizes (90 nm and 24 nm). Under laminar flow at 75 °C, the effect of inlet fluid temperature on heat transfer characteristics is investigated using a hybrid nanofluid of SiC/Al<sub>2</sub>O<sub>3</sub> with two concentrations of 0.1 vol.% and 0.2 vol.%. The dimensions of the radiator are given in tab. 2.

The nanofluid volume concentration and the hot and cold circuit flow parameters in the present investigation are given in tab. 3.

Table 2. Measurements of the radiator

Parameter	Dimensions [cm]
Length of radiator	34
Width of radiator	1.7
Height of radiator	31
Thickness of fin	0.01
Length of fin	1.1
Number of tubes	42
Length of tube	32
Thickness of tube	0.007
Hydraulic diameter of tube	0.373

Table 3. Experimental testing conditions of nanofluids

Parameters	Variation in parameters
Al <sub>2</sub> O <sub>3</sub> /SiC-L [vol.%]	0.1 and 0.2
Al <sub>2</sub> O <sub>3</sub> /SiC-S [vol.%]	0.1 and 0.2
Mass-flow rate of nanofluid [gs <sup>-1</sup> ]	13, 26, 39, 52 & 65
Experimental parameters	$T_{in}$ , $T_{out}$ , $T_a$ , $T_b$ , and $T_w$
Nanofluid inlet temperature [°C]	75
Air velocity [ms <sup>-1</sup> ]	1, 2, 3, 4, and 5



### Data processing

The following equations are used to investigate thermophysical parameters including, viscosity, thermal conductivity and density, which are essential in determining particle size effect.

Graham's eq. (1) shows that particle size has less influence on the viscosity of a fluid:

$$\frac{\mu_{nf}}{\mu_{bf}} = 1 + 2.5\varphi + \left[ \frac{1}{\left(\frac{h_p}{d_p}\right) \times \left(2 + \frac{h_p}{d_p}\right) \times \left(1 + \frac{h_p}{d_p}\right)} \right] \quad (1)$$

The density of the nanofluids are calculated by eq. (2):

$$\rho_{h,nf} = \varphi_{s1}\rho_{s1} + \varphi_{s2}\rho_{s2} + \rho_{nf}(1 - \varphi_s) \quad (2)$$

where  $\varphi_s$  is the total volume concentration of hybrid nanofluid,  $\rho_s$  – the density of the first nanoparticle, and  $\rho_{s2}$  – the density of the second nanoparticle.

The viscosity of the nanofluid is calculated for low particle volume concentration from the Einstein model of eq. (3):

$$\mu_{h,nf} = \frac{\mu_{nf}}{(1 - \varphi_{s1})^{2.5} (1 - \varphi_{s2})^{2.5}} \quad (3)$$

The Maxwell model is used to calculate thermal conductivity in eq. (4):

$$\frac{k_{h,nf}}{k_{bf}} = \frac{k_{s2} + (n-1)k_{bf} - (n-1)\varphi_2(k_{bf} - k_{s2})}{k_{s2} + (n-1)k_{bf} + \varphi_2(k_{bf} - k_{s2})} \quad (4)$$

where

$$\alpha = \frac{k_p}{k_f}$$

Equation (5) is used to calculate the heat transfer coefficient:

$$h = \frac{\dot{m}C_p(T_{in} - T_{out})}{A[T - T_w]} \quad (5)$$

The peripheral area is given by:

$$A = 2[lh + lw] \quad (6)$$

where  $l$  is the length,  $w$  – the width, and  $h$  – the height of the tube.

Equation (7) gives the Reynolds number:

$$Re = \frac{\rho v d}{\mu} \quad (7)$$

Equation (8) gives the Nusselt number:

$$Nu = \frac{hd}{k} \quad (8)$$

Equation (9) is used to calculate the hydraulic diameter of tubes:

$$d = \frac{4A'}{P} \quad (9)$$

Equation (10) is used to calculate the friction factor of laminar flow:

$$f = \left( \frac{\Delta p}{\frac{\rho v^2}{2}} \right) \frac{d}{l} \quad (10)$$

## Results and discussions

### Analysis of heat transfer characteristics

Experiments are conducted with Al<sub>2</sub>O<sub>3</sub>/SiC-L, Al<sub>2</sub>O<sub>3</sub>/SiC-S with 0.1 vol.%, and Al<sub>2</sub>O<sub>3</sub>/SiC-L, Al<sub>2</sub>O<sub>3</sub>/SiC-S with 0.2 vol.% under laminar flow conditions at 75 °C in the present study. Heat transfer characteristics like heat transfer coefficient, Nusselt number, and friction factor with Reynolds number are drawn for hybrid nanofluids. The findings are examined based on particle size, volume concentration, and flow rate.

### Analysis of heat transfer coefficient for hybrid nanofluids under laminar flow

Figure 10 shows the heat transfer coefficient for hybrid nanofluids at 75 °C as a function of Reynolds number. Al<sub>2</sub>O<sub>3</sub>/SiC-S with a 0.2 vol.% content showed a higher heat transfer coefficient at all Reynolds number ranges. The maximum heat transfer coefficient is obtained for Al<sub>2</sub>O<sub>3</sub>/SiC-S at 0.2 vol.% is 1317 w/m<sup>2</sup>k at Reynolds number of 1800. Further, the heat transfer coefficient is 5.3% higher than Al<sub>2</sub>O<sub>3</sub>/SiC-L of 0.1 vol.% and 6.4% than base fluid. This is due to the reduction of particle size in the hybrid nanofluids. The enhancement in thermal conductivity is affected by the clustering and aggregation, reduced largely by milling and nanoparticles' size. With the reduction in particulate size by milling, the hybrid nanofluid's heat transfer coefficient increases by 9-11%.

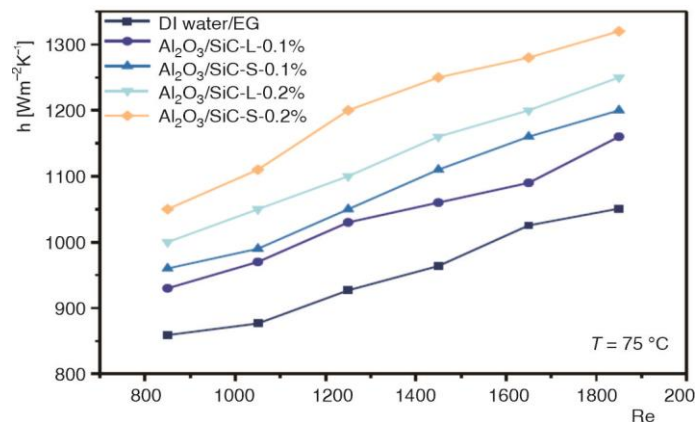


Figure 10. Variation of heat transfer coefficient with Reynolds number

It is observed that Al<sub>2</sub>O<sub>3</sub>/SiC-S has a higher heat transfer coefficient than Al<sub>2</sub>O<sub>3</sub>/SiC-L at a higher flow rate. This is due to the enlarged surface area of smaller particles and more particles present in the nanofluids. An increase in the heat transfer coefficient is observed as the particles' distribution is uniform for smaller particles than larger particles at a higher flow rate. The interactions between the smaller SiC-S particles with the Al<sub>2</sub>O<sub>3</sub> are higher than the

larger SiC-S particles with the  $\text{Al}_2\text{O}_3$ , increasing chaotic movements and dispersions and enhancing the heat transfer coefficient. The average increase in the heat transfer coefficient of the nanofluid when the particle size is reduced is found to be between 15% and 42 %.

*Analysis of Nusselt number for hybrid nanofluids under laminar flow*

Figure 11 shows the variation of Nusselt number with Reynolds number for hybrid nanofluids at 75 °C. It is seen from the graph that Nusselt number increases with flow rate and concentration. Concerning concentration, the Nusselt number for  $\text{Al}_2\text{O}_3/\text{SiC-S}$  at 0.2 vol.% is 31 at Reynolds number of 1800, and it is 2.5% higher than  $\text{Al}_2\text{O}_3/\text{SiC-L}$  of 0.1 vol.% and 3.5% higher than base fluid. The maximum Nusselt number obtained for  $\text{Al}_2\text{O}_3/\text{SiC-S}$  at 0.2 vol.% is due to smaller nanoparticles, making a large surface area, and low agglomerates than larger nanoparticles. The  $\text{Al}_2\text{O}_3/\text{SiC-S}$  has a higher Nusselt number than  $\text{Al}_2\text{O}_3/\text{SiC-L}$  at a higher flow rate from large and smaller particles. This is because of smaller particles' enlarged surface area and more number of particles than larger nanoparticles. An average enhancement of Nusselt number of 7-12% is observed for  $\text{Al}_2\text{O}_3/\text{SiC-S}$  due to increased thermal conductivity. A maximum Nusselt number enhancement of 2.8% is observed for  $\text{Al}_2\text{O}_3/\text{SiC-S}$ , which is 8% higher than  $\text{Al}_2\text{O}_3/\text{SiC-L}$ . The Nusselt number enhancement for smaller nanoparticles is because of low viscosity, large surface area, and low agglomerates than the larger nanoparticles.

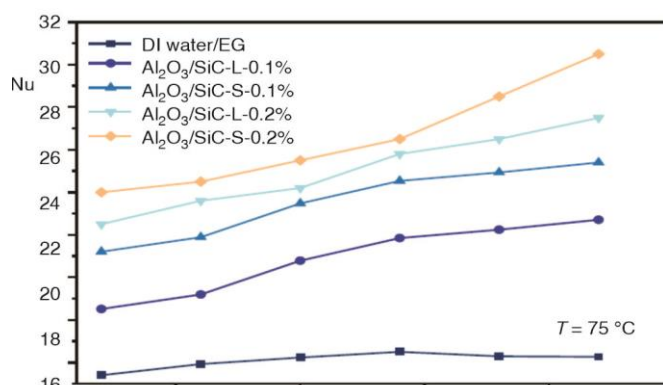


**Figure 11. Variation of Nusselt number with Reynolds number**

Following a similar trend, the Nusselt number of the nanofluid increases gradually as the Reynolds number and volume concentration increase. By increasing the concentration of nanoparticles in the nanofluid, convective heat transmission may be improved. This may be because adding nanoparticles to a fluid changes the flow structure.

*Analysis of friction factor for hybrid nanofluids under laminar flow*

The variation of friction factor with Reynolds number at 75 °C is shown in fig.12. The friction factor lowers as the flow rate increases and increases as concentration decreases. The friction factor for  $\text{Al}_2\text{O}_3/\text{SiC-L}$  of 0.2 vol.% is 2.6% higher than  $\text{Al}_2\text{O}_3/\text{SiC-L}$  of 0.1 vol.% and 3.2% higher than base fluid concerning volume concentration. The increase of friction factor is higher for hybrid nanofluids with increasing volume concentration. It is seen that  $\text{Al}_2\text{O}_3/\text{SiC-L}$  at 0.2 vol.% has the highest friction factor due to the presence of larger nanoparticles.

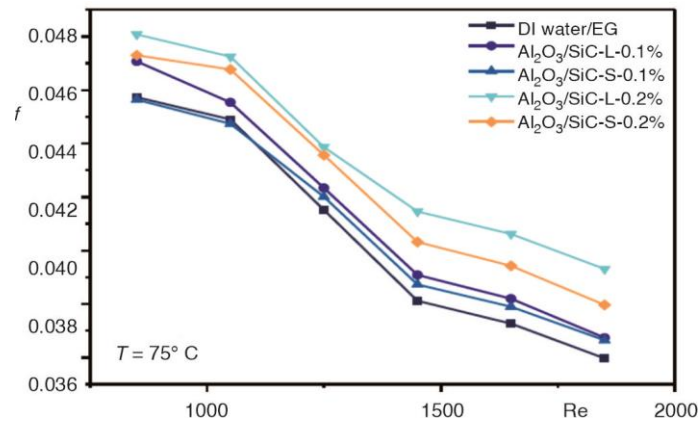


**Figure 12.** Variation of friction factor with Reynolds number

The  $\text{Al}_2\text{O}_3/\text{SiC-L}$  has a higher friction factor for large and smaller particles than  $\text{Al}_2\text{O}_3/\text{SiC-S}$  at a higher flow rate. An average enhancement of 9-12% is observed for  $\text{Al}_2\text{O}_3/\text{SiC-S}$  due to increased viscosity. It is also observed that  $\text{Al}_2\text{O}_3/\text{SiC-L}$  at 0.2 vol.% shows a higher friction factor than  $\text{Al}_2\text{O}_3/\text{SiC-S}$  at 0.2 vol.% at all Reynolds number. This is because of bigger nanoparticles and more agglomeration during the flow of nanofluids. A maximum friction factor enhancement of 2.9% is observed for  $\text{Al}_2\text{O}_3/\text{SiC-L}$  at 0.2 vol.%, which is 6% higher than  $\text{Al}_2\text{O}_3/\text{SiC-S}$  at 0.1 vol.%, proving smaller nanofluids have better flow than larger nanofluids. The increase in Reynolds number influences the friction factor, and the average increase of friction factor is minor, which can be negligible.

#### *Correlations for hybrid nanofluids under laminar flow*

A correlation equation for the Nusselt number was developed for laminar flow using the experimental values and regression analysis. The correlation of the nanofluids flowing through the radiator with the Reynolds number range of  $700 < \text{Re} < 2200$ ,  $\varphi = 1\%$ ,  $11.93 < \text{Pr} < 18.46$  is given:

$$\text{Nu}_{\text{reg}} = 0.5637 \text{Re}^{0.7851} \text{Pr}^{0.4} (1 + \varphi)^{0.2362} \quad (11)$$

As shown in fig. 13, the Nusselt number values obtained from the regression equations are compared to the experimental results. With a standard deviation of 6.3% and an average deviation of 5.4%, this implies that the predicted values match the actual values of laminar flow. To predict the friction factor under laminar flow circumstances, a regression equation is developed and provided by eq. (12). In the radiator, the hybrid nanofluid is flowing in the range of  $700 < \text{Re} < 2200$ ,  $\varphi = 1\%$  laminar conditions:

$$f_{\text{reg}} = 24.83 \text{Re}^{-0.6352} (1 + \varphi)^{0.1969} \quad (12)$$

The friction factor experimental findings are compared to the regression equation values in fig. 14. The regression friction factor and the experimental friction factor for laminar flow are linear, with a standard deviation of 5.9% and an average variance of 4.8%.

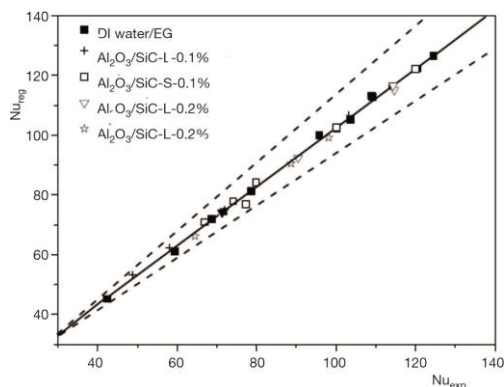


Figure 13. Comparison of experimental and correlated Nusselt number values

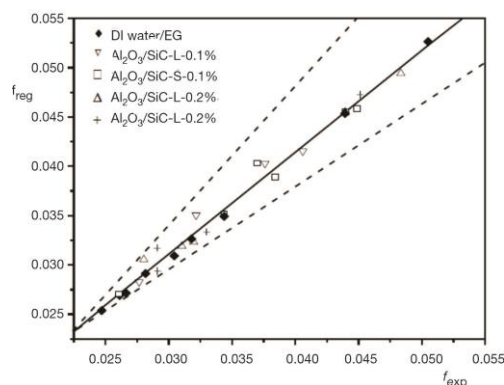


Figure 14. Comparison of experimental and friction factor values

### Conclusion

The  $\text{Al}_2\text{O}_3/\text{SiC-S}$  of 0.2 vol.% is 2.1% shows a higher heat transfer coefficient than  $\text{Al}_2\text{O}_3/\text{SiC-L}$  of 0.1 vol.% and 2.8% higher than base fluid based on particle size and volume concentration, Small-sized nanoparticles in the  $\text{Al}_2\text{O}_3/\text{SiC-S}$  create a large surface area and uniform distribution of the nanofluid flowing through the radiator tubes.

Nusselt number for  $\text{Al}_2\text{O}_3/\text{SiC-S}$  of 0.2 vol.% is 2.7% higher than  $\text{Al}_2\text{O}_3/\text{SiC-L}$  of 0.1 vol.% and 3.2% higher than base fluid. The chaotic movement is increased in the presence of more molecules than larger nanoparticles because of the increase in Nusselt number.

The friction factor for  $\text{Al}_2\text{O}_3/\text{SiC-S}$  of 0.2 vol.% is 4.3% lower than  $\text{SiC-L}$  of 0.3 vol.% and 1.5% higher than base fluid. The friction factor decreases at a higher velocity and can be negligible compared to the base fluid.

Nanofluids with smaller sizes show higher heat transfer characteristics than larger sizes in laminar flow conditions. The heat transfer characteristics are higher for hybrid nanofluids because of more particles, two different particles, and a large surface area.

### Acknowledgment

This study is supported by Taif University Researchers Supporting Project number (TURSP-2020/49), Taif University, Taif, Saudi Arabia. The authors would like to thank Taif University for its financial support.

### Nomenclature

$h_{ip}$  – particle interspacing  
 $H$  – heat transfer coefficient  
 $T_{in}$  – inlet temperature of nanofluid  
 $T_{out}$  – outlet temperature of nanofluid

Greek symbol  
 $\varphi$  – concentration [%]

### References

- [1] Goudarzi, K., Jamali, H., Heat Transfer Enhancement of  $\text{Al}_2\text{O}_3$ -EG Nanofluid in a Car Radiator with Wire Coil Inserts, *Applied Thermal Engineering*, 118 (2017), C, pp. 510-517
- [2] Devireddy, S., et al., Improving the Cooling Performance of Automobile Radiator with Ethylene Glycol Water Based  $\text{TiO}_2$  Nanofluids, *Int Comm. in Heat and Mass Transfer*, 78 (2016), Nov., pp. 121-126
- [3] Elsebay, M., et al., Numerical Resizing Study of  $\text{Al}_2\text{O}_3$  and CuO Nanofluids in the Flat Tubes of a Radiator, *Applied Mathematical Modelling*, 40 (2016), 13-14, pp. 6437-6450

- [4] Nieh, H. M., et al., Enhanced Heat Dissipation of a Radiator Using Oxide Nano-Coolant, *International Journal of Thermal Sciences*, 77 (2014), Mar., pp. 252-261
- [5] Elias, M. M., et al., Experimental Investigation on the Thermo-Physical Properties of Al<sub>2</sub>O<sub>3</sub> Nanoparticles Suspended in Car Radiator Coolant, *International Communications in Heat and Mass Transfer*, 54 (2014), May, pp. 48-53
- [6] Hussein, A. M., et al., Heat Transfer Enhancement Using Nanofluids in an Automotive Cooling System, *International Communications in Heat and Mass Transfer*, 53 (2014), Apr., pp. 195-202
- [7] Peyghambarzadeh, S. M., et al., Experimental Study of Overall Heat Transfer Coefficient in the Application of Dilute Nanofluids in the Car Radiator, *Applied Thermal Eng.*, 52 (2013), 1, pp. 8-16
- [8] Vajjha, R. S., et al., Numerical Study of Fluid Dynamic and Heat Transfer Performance of Al<sub>2</sub>O<sub>3</sub> and CuO Nanofluids in the Flat Tubes of a Radiator, *International Journal of Heat and Fluid Flow*, 31 (2010), 4, pp. 613-621
- [9] Leong, K. Y., et al., Performance Investigation of an Automotive Car Radiator Operated with Nanofluid-Based Coolants (Nanofluid as a Coolant in a Radiator), *Applied Thermal Engineering*, 30 (2010), 17-18, pp. 2685-2692
- [10] Jasim, Q. K., et al., Improving Thermal Performance Using Al<sub>2</sub>O<sub>3</sub>-Water Nanofluid in a Double Pipe Heat Exchanger Filling with Porous Medium, *Thermal Science*, 24 (2020), 6B, pp. 4267-4275
- [11] Zhen, D., et al., Heat Transfer Performance and Friction Factor of Various Nanofluids in a Double-Tube Counter Flow Heat Exchanger, *Thermal Science*, 24 (2020), 6A, pp. 3601-3612
- [12] Qamar, A., et al., Dispersion Stability and Rheological Characteristics of Water and Ethylene Glycol Based ZnO Nanofluids, *Thermal Science*, 25 (2021), 3A, pp. 1989-2001
- [13] Arulprakasajothi, M., et al., Performance Study of Conical Strip Inserts in Tube Heat, *Thermal Science*, 22 (2018), 1B, pp. 477-485
- [14] Topuz, A., et al., Determination and Measurement of Some Thermophysical Properties of Nanofluids and Comparison with Literature Studies, *Thermal Science*, 25 (2021), 5A, pp. 3579-3594
- [15] Selvam, C., et al., Overall Heat Transfer Coefficient Improvement of an Automobile Radiator with Graphene-Based Suspensions, *Int. Journal of Heat and Mass Transfer*, 115 (2017), Part B, pp. 580-588
- [16] Elsaid, A. M., Experimental Study on the Heat Transfer Performance and Friction Factor Characteristics of CO<sub>3</sub>O<sub>4</sub> and Al<sub>2</sub>O<sub>3</sub> Based H<sub>2</sub>O/(CH<sub>2</sub>OH)<sub>2</sub> Nanofluids in a Vehicle Engine Radiator, *International Communications in Heat and Mass Transfer*, 108 (2019), 104263
- [17] Cardenas Contreras, E. M., et al., Experimental Analysis of the Thermohydraulic Performance of Graphene and Silver Nanofluids in Automotive Cooling Systems, *International Journal of Heat and Mass Transfer*, 132 (2019), Apr., pp. 375-387
- [18] Kocak Soylu, S., et al., Improving Heat Transfer Performance of an Automobile Radiator Using Cu and Ag Doped TiO<sub>2</sub> Based Nanofluids, *Applied Thermal Engineering*, 157 (2019), July, 113743
- [19] Singh Sokhal, G., et al., Influence of Copper Oxide Nanoparticles on the Thermophysical Properties and Performance of Flat Tube of Vehicle Cooling System, *Vacuum*, 157 (2018), Nov., pp. 268-276
- [20] Tijani, A. S., Sudirman, A. S., Thermo-Physical Properties and Heat Transfer Characteristics of Water/Anti-Freezing and Al<sub>2</sub>O<sub>3</sub>/CuO Based Nanofluid as a Coolant for Car Radiator, *International Journal of Heat and Mass Transfer*, 118 (2018), Mar., pp. 48-57
- [21] Moghaieb, H. S., et al., Engine Cooling Using Al<sub>2</sub>O<sub>3</sub>/Water Nanofluids, *Applied Thermal Engineering*, 115 (2017), Mar., pp. 152-159
- [22] Oliveira, G. A., et al., Experimental Study on the Heat Transfer of MWCNT/Water Nanofluid Flowing in a Car Radiator, *Applied Thermal Engineering*, 111 (2017), Jan., pp. 1450-1456